ISSN 1000-9825, CODEN RUXUEW
Journal of Software, Vol.17, No.4, April 2006, pp.729−739
DOI: 10.1360/jos170729

E-mail: jos@iscas.ac.cn
http://www.jos.org.cn
Tel/Fax: +86-10-62562563

二维 Logistic 映射的动力学分析*

王兴元+, 骆 超

(大连理工大学 电子与信息工程学院,辽宁 大连 116024)

Dynamic Analysis of the Coupled Logistic Map

WANG Xing-Yuan+, LUO Chao

(School of Electronic and Information Engineering, Dalian University of Technology, Dalian 116024, China)

+ Corresponding author: Phn: +86-411-82056240, Fax: +86-411-84708918, E-mail: wangxy@dlut.edu.cn

Wang XY, Luo C. Dynamic analysis of the coupled logistic map. *Journal of Software*, 2006,17(4):729−739.
http://www.jos.org.cn/1000-9825/17/729.htm

Abstract: Dynamic analysis of the coupled logistic map redounds to know and predict the characteristics of high-dimension complex nonlinear system. Using the method combining calculation and experiment, the following conclusions are shown: (1) The boundary equation of the first bifurcation of the coupled logistic map in the parameter space is given out. (2) Chaotic patterns of the coupled logistic map may emerge out of double-periodic bifurcation and Hopf bifurcation, respectively. (3) The boundary between periodic and non-periodic regions in the attraction basin of the coupled logistic map is fractal, which indicates the impossibility to predict the moving result of the points in phase plane. (4) The structures of the Mandelbrot-Julia sets are determined by the control parameters, and their boundaries have the fractal characteristic.
Key words: coupled logistic map; bifurcation; chaos; Mandelbrot-Julia set; fractal

摘 要: 对二维 logistic 映射的动力学研究有助于认识和预测更复杂的高维非线性系统的性态.利用解析计算和实验分析相结合的方法揭示出:(1) 参数空间中二维 logistic 映射发生第一次分岔的边界方程;(2) 二维 logistic 映射可按倍周期分岔和 Hopf 分岔走向混沌;(3) 二维 logistic 映射的吸引盆中周期和非周期区域之间的边界是分形的,这意味着无法预测相平面上点运动的归宿;(4) Mandelbrot-Julia 集的结构由控制参数决定,且它们的边界是分形的.
关键词: 二维 logistic 映射;分岔;混沌;Mandelbrot-Julia 集;分形
中图法分类号: TP301 文献标识码: A

1 Introduction

May, the mathematical ecologist, has suggested in one of his influential article published in 1976 by “Nature”,

* Supported by the National Natural Science Foundation of China under Grant No.60573172 (国家自然科学基金); the Superior College Science Technology Research Project of Liaoning Province of China under Grant No.20040081 (辽宁省教育厅高等学校科学技术研究计划)

Received 2004-04-22; Accepted 2005-05-31

that the non-heterogamous insect population model in ecology can be explained in terms of nonlinear difference equation[1]

$$x_{n+1} = \mu x_n (1 - x_n) \tag{1}$$

According to the study on the logistic map, people have found that it come through double-periodic bifurcation into the chaos[2]. Based on this foundation, people have studied the chaos of the two-dimension logistic map and its application in ecology, etc[3]. For example, Satoh and Aihara have studied self-similarity of the attractor for a two-dimension predator-prey system[4]; According to chaotic dynamics of the coupled logistic map, Hastings has investigated the fluctuation of insect and population[5], and Zengru and Sanglier have analyzed the interaction of demand and supply in economics[6]. What kinds of dynamic characteristics does the coupled logistic map with a simple coupling term have?

$$\begin{cases} x_{n+1} = x_n + h(x_n - x_n^2 + y_n) \\ y_{n+1} = y_n + h(y_n - y_n^2 + x_n) \end{cases} \tag{2}$$

Therefore, this paper gives a careful study on the dynamic behaviors of Eq.(2).

2 Bifurcation Theory of the Coupled Logistic Map

Eq.(2) can be expressed as $\vec{Z}_{n+1} = f(\vec{Z}_n)$. Assume $\vec{Z}_* = (x_*, y_*)$ is the fixed point of Eq.(2), then $\vec{Z}_*$=(x_*,y_*) is the solution to the equations below:

$$\begin{cases} x_* = x_* + h(x_* - x_*^2 + y_*) \\ y_* = y_* + h(y_* - y_*^2 + x_*) \end{cases} \tag{3}$$

From Eq.(3), we can get the fixed points as $(\vec{Z}_*)_1 = (0,0)$ and $(\vec{Z}_*)_2 = (2,2)$.

The stability of these fixed points is relative to the maximum eigenvalue (its absolute value is expressed as $|K|_{\max}$) of Jacobi matrix on the fixed points. If $f'(\vec{Z}_*)$ is expressed as the Jacobi matrix of the map f on the fixed points, then

$$f'(\vec{Z}_*) = \left.\frac{\delta f}{\delta \vec{Z}}\right|_{\vec{Z}=\vec{Z}_*} = \begin{bmatrix} 1+h-2hx_* & h \\ h & 1+h-2hy_* \end{bmatrix}.$$

If $|K|_{\max}<1$, then the fixed points are stable; If $|K|_{\max}>1$, then the fixed points are unstable; If $|K|_{\max}=1$, the first bifurcation of Eq. (2) will occur[7]. We calculate the solutions of the characteristic polynomial of $f'(\vec{Z}_*)$ and get two eigenvalues as follows:

$$\begin{cases} K_+ = \frac{1}{2}(L + \sqrt{M^2 + 4N}) \\ K_- = \frac{1}{2}(L - \sqrt{M^2 + 4N}) \end{cases} \tag{4}$$

where $L=2+2h-2h(x_*+y_*)$,$M=2h(y_*-x_*)$,$N=h^2$, then

$$|K|_{\max} = \begin{cases} K_+ & \text{if} \quad 2+2h-2h(x_*+y_*) > 0 \\ K_- & \text{if} \quad 2+2h-2h(x_*+y_*) < 0 \end{cases} \tag{5}$$

Eq.(5) shows that $|K|_{\max}$ is the function of parameter h. According to condition $|K|_{\max}=1$, using Eq.(5), we can deduce the boundary of Eq.(2) in parameter space when the first bifurcation occurs

$$(1+h-2hx_* \mp 1)(1+h-2hy_*) - h^2 + 1 \mp (1+h-2hx_*) = 0 \tag{6}$$

where "–" corresponds to $|K|_{\max}=K_+$, "+" corresponds to $|K|_{\max}=K_-$ in "$\mp$".

Substituting $(\vec{Z}_*)_1 = (0,0)$ into Eq.(4), we can deduce that this fixed point is unstable. Substituting $(\vec{Z}_*)_2 = (2,2)$ into Eq.(6), we can deduce that if h=0, then the first bifurcation of Eq.(2) will occur when $h<1/3$; if

h=1 or h=1/2, then the first bifurcation of Eq.(2) will occur when h>1/3.

3 Experiment and Results

The dynamic behavior of Eq.(2) is determined by the control parameter h. In order to make full study of the behavior of Eq.(2) in the parameter space, the authors use a few methods such as phase graph, bifurcation graph, power spectra, Lyapunov exponent, correlation dimension, and attraction basin to study the evolution of the systemic behavior with the change of parameter along the two paths in the parameter space.

3.1 Bifurcation process

3.1.1 Analysis of phase graph and bifurcation graph

The two paths in the parameter space are $h\in[-1.35,-0.98]$ and $h\in[0.497,0.686]$ respectively. Choosing the initial point (x_n,y_n)=(0.4,0.5), the authors construct the attractor and bifurcation graph of Eq.(2). Fig.1 and Fig.2 show a group of representative results.

Let us observe the evolution of the systemic behavior with the change of parameter h along the first path: When $-0.9995\le h\le -0.98$, the system converges to a fixed point in the phase plane (shown as Fig.2(a)); Decreasing h, when $-1.22445\le h\le -0.99951$, $-1.27195\le h\le -1.22446$, $-1.28216\le h\le -1.27196$, $-1.28436\le h\le -1.28217$, …, etc, the system takes place double-periodic bifurcation and appears in turn 2 points, 4 points, 8 points and so on in the phase plane (shown as Fig.2(a)); Continuing decreasing h, when $-1.31327\le h\le -1.28498$ chaos appears; Decreasing h, when $-1.31518\le h\le -1.31328$, periodic-6 points emerge in phase plane (Fig.2(b)); Continuing decreasing h again, when $-1.31608\le h\le -1.31519$, $-1.3163\le h\le -1.31609$, $-1.31634\le h\le -1.31631$, …, etc, the system takes place double-periodic bifurcation again and appears in turn 12 points, 24 points, 48 points and so on in the phase plane (Fig.2(b)); Decreasing h, when $-1.35\le h\le -1.31637$ chaos emerges again (Fig.2(b)).

The evolution of systematic behavior when the control parameter h varies along the second path is as follows: When $0.497\le h\le 0.49973$, the system tends to a stable fixed point in the phase plane (Fig.2(c)); Increasing h, when $0.49974\le h\le 0.50012$, two fixed points emerge in the phase plane (Fig.2(c)); When $0.50013\le h\le 0.50022$, a limit loop appears in the phase plane (Fig.2(c)); When $0.50023\le h\le 0.5997$, two stable fixed points emerge in the phase plane again (Fig.1(a)); When $0.5998\le h\le 0.65286$, the two fixed points are unstable and the new stability state is two limit loops around the former fixed points (Fig.1(b)), moreover, these two limit loops will increasedly deform with h increasing (Fig.1(c)). Fig.1(b) and Fig.1(c) show that the two stable limit loops are closed, and their neighboring orbits converge on them. Continuing increasing h, when $0.65287\le h\le 0.686$, further bifurcation will occur and strange attractors emerge in phase plane (Fig.1(d)~Fig.1(f), Fig.2(d)).

According to the attractor and its partial magnification (from Fig.1(f) to Fig.1(h)), we can see that strange attractors refer to a sort of movement with unrepeated orbit and complicated properties, which is restricted in limited region all along. The delicate structure of strange attractor exists by all scales, and the strange attractors wouldn't form entity in the phase space even in the infinite time limit.

Property 1. The attractor in Fig.1 is symmetry about beeline $y=x$.

Proof. Using the inductive method of mathematics. Let $z_n=x_n+y_n^i$, $z_n^*=y_n+x_n^i$, then Eq.(2) may be denoted as $z_{n+1}=f(z_n)$. From Eq.(2), we can know

$$f^*(z_n)=f(z_n^*).$$

Suppose $[f^{k-1}(z_n)]^*=f^{k-1}(z_n^*)$ is tenable.

because $[f^k(z_n)]^*=[f^{k-1}[f(z_n)]]^*=f^{k-1}[f(z_n)]^*=f^{k-1}[f^*(z_n)]=f^{k-1}[f(z_n^*)]=f^k(z_n^*)$.

Namely, $[f^k(z_n)]^*=f^k(z_n^*)$ (k=1,2,…,N; N refers to the times of iteration), it demonstrates that the attractors constructed by Fq.(2) are symmetry about beeline $y=x$.

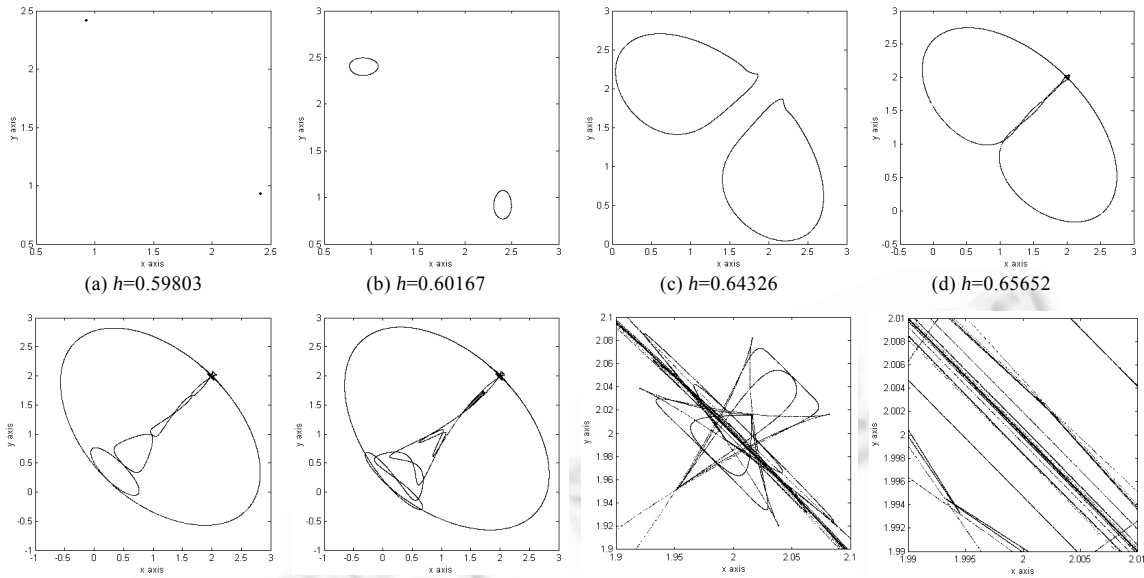

(a) h=0.59803 (b) h=0.60167 (c) h=0.64326 (d) h=0.65652

(e) h=0.68011 (f) h=0.6845 (g) Partial enlargement of Fig.1(f) (h) Partial enlargement of Fig.1(g)

Fig.1 Attractors of Eq.(2)

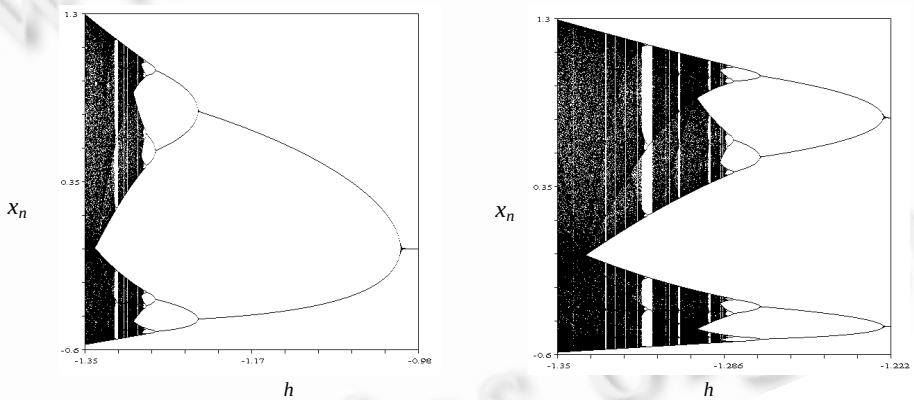

(a) The parameter varies along the first path (b) Partial enlargement of Fig.2(a)

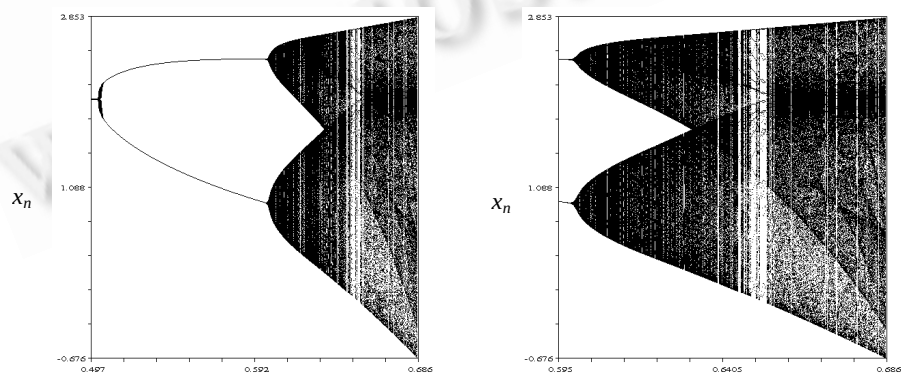

(c) The parameter varies along the second path (d) Partial enlargement of Fig. 2(c)

Fig.2 Bifurcation graphs of Eq.(2)

The period doubling, fixed point, limit loop and strange attractor are observed in the two ways to chaos

mentioned above. It indicates that Eq.(2) will tend to chaos through double-periodic bifurcation or Hopf bifurcation, respectively[8].

In 1978, using the method of renormalization group, Feigenbaum found that the interval ratio limit δ=4.66920 in convergence sequence of bifurcation value μ_n (n=1,2,…) is a universal constant when Eq.(2) turns into chaos through double-periodic bifurcation. This constant is known as Feigenbaum constant that reflect the regularity of the way by which the system turns into chaos through double-periodic bifurcation[2]. Using the method combining calculation and experiment, the authors get the interval ratio limit in the convergence sequence of bifurcation value h_n (n=1,2,…) and h_m (m=1,2,…) which twice the double-periodic bifurcation emerge successively in the first way to chaos we have discussed above

$$\delta' = \lim_{n\to\infty} \frac{h_n - h_{n-1}}{h_{n+1} - h_n} = 4.48391... \tag{7}$$

$$\delta'' = \lim_{n\to\infty} \frac{h_m - h_{m-1}}{h_{m+1} - h_m} = 4.37846... \tag{8}$$

From Eq.(7) and Eq.(8), it can be found that δ' and δ'' are almost equal to Feigenbaum constant δ. This indicates that the logistic map and the coupled logistic map have some common rules: On the process of turning to chaos through a series of double-periodic bifurcations they all represent self-similarity and scale transform invariability in the parameter space and the phase space. This evolvement process is a generic characteristic in a nonlinear system.

3.1.2 Power spectra analysis

According to Welch's method of average periodic chart[9], the authors calculate the power spectra of Eq.(2). The data used in computing are the sequence values of x_n (n=1,2,3,…). The parameters used in the analysis are: sampling frequency 1Hz; FFT length M:1024; window type: rectangular window; window length L:1024; maximum number of analysis samples N:10000; segment number K:194. The authors calculate the power spectra corresponding to the attractor in Fig.1 (shown as Fig.3).

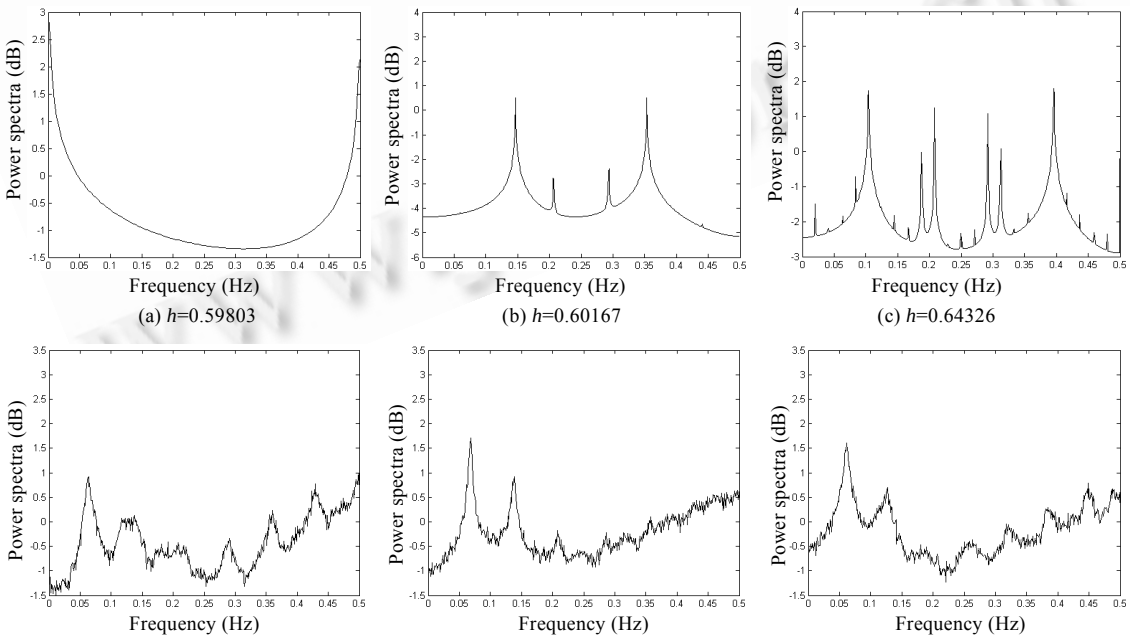

Fig.3 Power spectra of attractors of Eq.(2)

3.1.3 The computation of the Lyapunov exponent and the fractal dimension

According to the method of calculating Lyapunov exponents from difference equation[3], the authors calculate the variation curves of Lyapunov exponent λ_1 and λ_2 of Eq.(2) when the control parameter varies along the two paths mentioned above (Fig.4(a) and Fig.4(c)). In addition, when the two Lyapunov exponents of the coupled logistic map are $(\lambda_1,\lambda_2)=(+,-)$ the system is described by strange attractors, according to Kaplan-Yorke assumption[10]: $d=1-\lambda_1/\lambda_2$, we can get the fractal dimension d; when the Lyapunov exponents are $(\lambda_1,\lambda_2)=(-,-)$, the system tends to be a fixed point with fractal dimension $d=0$; when Lyapunov exponents are $(\lambda_1,\lambda_2)=(0,-)$, the system shows a limit loop with fractal dimension $d=1$[11,12]. Thus according to the change curve of Lyapunov exponent λ_1 and λ_2, the authors calculate its fractal dimension d of attractor of Eq.(2) when control parameter varies with the two paths mentioned above (Fig.4(b) and Fig.4(d)).

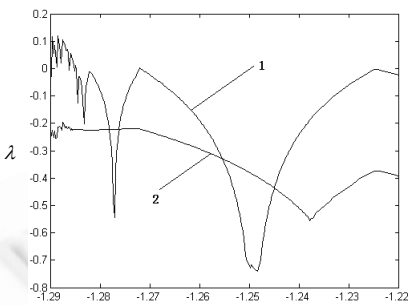

(a) Lyapunov exponent curve when parameter varies along the first path: $1-\lambda_1$, $2-\lambda_2$

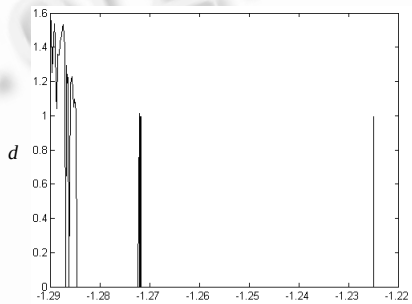

(b) Fractal dimension curve when parameter varies along the first path

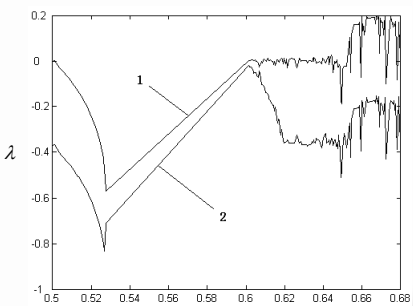

(c) Lyapunov exponent curve when parameter varies along the second path: $1-\lambda_1$, $2-\lambda_2$

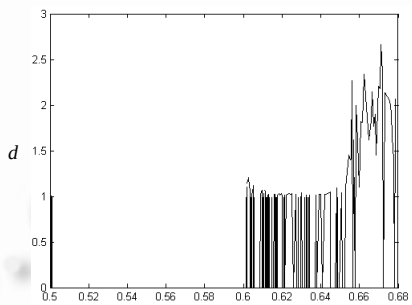

(d) Fractal dimension curve when parameter varies along the second path

Fig.4 Lyapunov exponent and fractal dimension curves of Eq.(2)

3.1.4 Attraction basin

The following two methods can be used to construct the attraction basin of Eq.(2): (1) Enacting the watch window W, the maximum iteration times N (here N=2000), and the value h exhibiting periodic-p movement (p is positive integer) of Eq.(2) in the phase space. (2) $\forall z_n=(x_n,y_n)\in W$,according to Eq.(2), calculate z_k. (3) Method I: if z_k ($k\le N$) falls into periodic-p orbit, then put point z_0 black, otherwise, put it white. Method II: if z_k ($k\le N$ and k is odd) falls in periodic-p orbit, then put point z_0 with black color, otherwise, put it with white color. (4) The course (2) and (3) are repeated, until all points in the watch window W are exhausted. Then we can get the periodic-p orbit attraction basin of Eq.(2).

Figure 5 shows the attraction basin of periodic-p orbit of Eq.(2). Figure 5(a) is generated with method I, and

Fig.5(b) and Fig.5(c) are generated with method II. The black and white region in Fig.5 represent the movement region of different characteristics respectively. For the initial points in black regions we can definitely predict that these points will finally evolve to periodic-p orbit with time changing. From partial enlargement of Fig.5(d), we can see that the boundary between black and white regions is fractal, i.e., there exists delicate structure to arbitrary minute scale. Thus we can conclude that the initial points of different characteristics in attraction basin are closely interwoven. Therefore, the final settling place of the movement is unpredictable, i.e., though Eq.(2) is described by periodic attractors in the phase space, the movement of points in the phase space is very complicated.

Theorem 1. Let $z_n = x_n + y_n^i$, $z_n^* = y_n + x_n^i$, then Eq.(2) may be denoted as $z_{n+1}=f(z_n)$. If the attraction basin is generated with Eq.(2), then we can get

$$[f^k(z_n)]^* = f^k(z_n^*) \ (k=1,2,\ldots,N).$$

Using the inductive method of mathematics, we can prove this theorem easily. Theorem 1 indicates that the attractor basin generated with Fq.(2) is symmetry about beeline $y=x$.

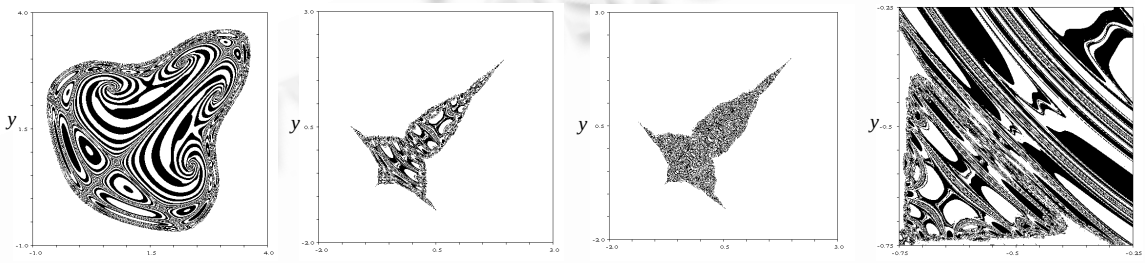

(a) Periodic-12 attraction basin for h=0.65136 (b) Periodic-4 attraction basin for h=−1.25296 (c) Periodic-8 attraction basin for h=−1.27651 (d) Partial enlargement of Fig.5(b)

Fig.5 Attraction basin of periodic orbit of Eq.(2)

3.2 Self-Similarity

Based on the "complex dynamic system theory" created by Julia and Faton, famous mathematician Mandelbrot not only construct the Julia set in the dynamical Z-plane and Mandelbrot set in parameter C-plane but also study them in 1970s[13]. Now people have done some deep study about Mandelbrot-Julia set and found out that there hides intricate regular structure in them, thus the fractal theory is enriched[14−16]. Based on the prediction made by Rössler in 1986 that the dynamic behavior of super-chaotic system in the phase space manifests in self-similarity[17], and the discovery given by Kaneko in 1983 that super-chaos phenomenon exists in the coupled logistic map[18], the fractal characteristics of self-similarity is discussed in this paper.

3.2.1 Mandelbrot-Julia sets in two-dimension space

The method to construct Mandelbrot-Julia set in two-dimension space is as follows: (1) Transform Eq.(2) into the following equation

$$\begin{cases} x_{k+1} = x_k + h_x(x_k - x_k^2 + y_k + c_x) \\ y_{k+1} = y_k + h_y(y_k - y_k^2 + x_k + c_y) \end{cases} \tag{9}$$

where the former one-dimension parameter h is replaced by two-dimension control parameters (h_x,h_y),c_x and c_y are two real parameters; (2) Enacting the watch window W ($W\subset C$ or Z), the escape-radius R and the escape-time limit N; (3) For Mandelbrot set, $\exists c_0\in W$ and $W\subset C$, let $z_0=(x_0,y_0)=(0,0)$ and choose the parameters h_x and h_y, then calculate z_k; For Julia set, $\exists z_0\in W$ and $W\subset Z$, choose the parameters c_x, c_y, h_x and h_y, then calculate z_k; (4) If after oddtimes of iteration, $|z_k| = \sqrt{x_k^2 + y_k^2} > R$ is satisfied, then put point z_0 with black color; otherwise, put point z_0 with white

color; (5) Steps (3) and (4) are repeated until all points in the watch window W are exhausted. Then we can get the Mandelbrot-Julia sets of Eq.(2) in two-dimension space (Fig.6).

Figure 6 shows that: (1) All kinds of the white strip regions outside of the black attracted region in Fig.6 are surrounded circuitously. Owing to the limited degree of precision of computer, the boundary of finite attracted region doesn't exhibit fractal property, however, when increasing the magnifying multiple, the delicate structure of the boundary curve of infinite attracted region exists by all scales, and it exhibits fractal property (Fig.6(b) and Fig.6(d)); (2) Fig.6 is symmetry about beeline $y=x$, and the proof of its symmetry is as follows:

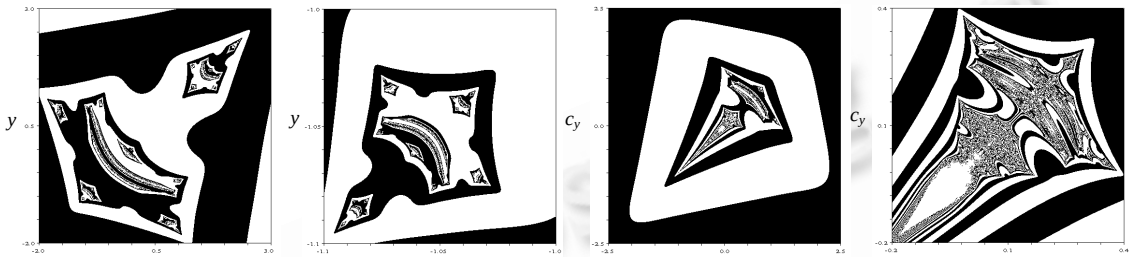

(a) Julia set, $c_x=c_y=0.8$, $h_x=h_y=-1.32997$ (b) Partial enlargement of Fig.6(a) (c) Mandelbrot set, $h_x=h_y=-1.32997$ (d) Partial enlargement of Fig.6(c)

Fig.6 Mandelbrot-Julia set of Eq.(2) in two-dimension space

Theorem 2. Let $z_n=x_n+y_n^i$, $z_n^*=y_n+x_n^i$, $c=c_x+c_y^i$ and $c^*=c_y+c_x^i$, then Eq.(9) may be denoted as $z_{n+1}=f(z_n)$. If the generalized Mandelbrot-Julia set is constructed by Eq.(9), then we can get

(i) $[f^k(z_n)]^*=f^k(z_n^*)$ (k=1,2,…,N). when $c_x=c_y$ and $h_x=h_y$.

(ii) $[f^k(c)]^*=f^k(c^*)$ (k=1,2,…,N). when $h_x=h_y$,.

Proof. (i) Using the inductive method of mathematics. From Eq.(9), when $c_x=c_y$ and $h_x=h_y$ we can get

$$f^*(z_n)=f(z_n^*).$$

Suppose $[f^{k-1}(z_n)]^*=f^{k-1}(z_n^*)$ is tenable.

$\because [f^k(z_n)]^*=[f^{k-1}[f(z_n)]]^*=f^{k-1}[f(z_n)]^*=f^{k-1}[f^*(z_n)]=f^{k-1}[f(z_n^*)]=f^k(z_n^*)$,

Namely, $[f^k(z_n)]^*=f^k(z_n^*)$ (k=1,2,…,N; N refers to the times of iteration), it demonstrates that the Julia sets constructed by Fq.(9) are symmetry about beeline $y=x$ (Fig.6(a)).

(ii) Similarity, when $h_x=h_y$ we can know $[f^k(c)]^*=f^k(c^*)$. It demonstrates that the Mandelbrot sets constructed by Fq.(9) are symmetry about beeline $y=x$ (Fig.6(c)).

So this proposition is tenable.

3.2.2 Two-dimension Julia set in four-dimension space

The plural form of Eq.(2)

$$\begin{cases} re(x_{n+1})=re(x_n)+h(re(x_n)-re(x_n)^2+im(x_n)^2+re(y_n)) \\ im(x_{n+1})=im(x_n)+h(im(x_n)-2re(x_n)im(x_n)+im(y_n)) \\ re(y_{n+1})=re(y_n)+h(re(y_n)-re(y_n)^2+im(y_n)^2+re(x_n)) \\ im(y_{n+1})=im(y_n)+h(im(y_n)-2re(y_n)im(y_n)+im(x_n)) \end{cases}$$

is a four-dimensional map and the Julia set of Eq.(10) is the point set of C^2 in four-dimensional space. Adopting the method that two variables are fixed, the authors focus on the projection of Julia set on another dynamic plane to find out its structure in four-dimensional maps. Using the time-escape algorithm[13] and choosing the escape-radius R=1000 and escape-time limit N=2000, the author constructs the two-dimensional projection of Julia set in four-

dimensional space (shown as Fig.7); the black represents the stable region and the white represents the escape region.

Figure 7 shows that: (1) The black stable region is embedded in the white escape region; (2) The structure of the Julia set varies with different control parameters. Figure 7(a) to Fig.7(c) are symmetry about beeline $y=x$ while Fig.7(d) is symmetry about the axis x; (3) Owing to the limited degree of precision of computer, the boundary of stable region doesn't exhibit fractal property, however, when increasing the magnifying multiple, the boundary of the stable region is smooth, and it exhibits fractal property (Fig.7(b)). The symmetry is proved as follows:

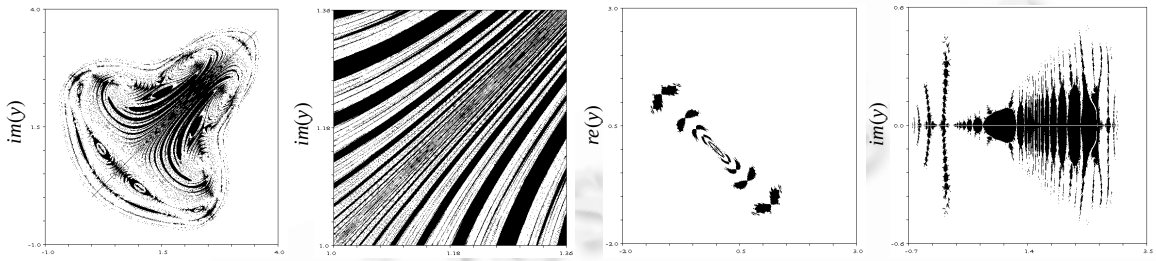

(a) $re(x_0)=re(y_0)=0.01$, $h=0.59635$ (b) Partial enlargement of Fig.7(a) (c) $im(x_0)=im(y_0)=0.01$, $h=0.65123$ (d) $im(x_0)=im(y_0),re(y_0)=-0.5$, $h=0.65123$

Fig.7 Two-Dimension Julia set of Eq.(2) in four-dimension space

Theorem 3. Let $z_n=(re(x_n),im(x_n),re(y_n),im(y_n))$, then Eq.(10) can be denoted as $z_{n+1}=f(z_n)$.

(i) If let $\eta_n=im(x_n)+im(y_n)i$, $\eta_n^*=im(y_n)+im(x_n)i$, then $[f^k(\eta_n)]^*=f^k(\eta_n^*)$ $(k=1,2,\ldots,N)$ when $re(x_0)=re(y_0)=a$ (a is real constant).

(ii) If let $\varepsilon_n=re(x_n)+re(y_n)i$, $\varepsilon_n^*=re(y_n)+re(x_n)i$, then $[f^k(\varepsilon_n)]^*=f^k(\varepsilon_n^*)$ $(k=1,2,\ldots,N)$ when $im(x_0)=im(y_0)=b$ (b is real constant).

(iii) If let $\delta_n=re(x_n)+im(y_n)i$, $\bar{\delta}_n=re(x_n)-im(y_n)i$, then $f^k(\delta_n)=\overline{f^k(\bar{\delta}_n)}$ $(k=1,2,\ldots,N)$ when $im(x_0)=im(y_0)$, $re(y_0)=a$ (a is real constant), or when $im(x_0)=a$, $re(y_0)=b$ (a, b are real constants).

On the basis of the conclusions (i) and (ii) drawn from Theorem 3, the Julia sets from Fig.7(a) to Fig.7(c) are symmetry about beeline $y=x$; and from conclusion (iii), the Julia set in Fig.7(d) is symmetry about the axis x.

4 Discussion and Conclusion

(1) From Fig.1 and Fig.2, we can see that when the control parameter varies, Eq.(2) comes through double-periodic bifurcation and Hopf bifurcation into chaos. The interval ratio limit of the bifurcation value sequence when the coupled logistic map takes place double-periodic bifurcation is almost the same as Feigenbaum constant. This reflects the regularity of the way by which the system turns into chaos through double-periodic bifurcation[19]. In order to testify this conclusion, further researches have been conducted in this field. For instance, Broucke made use of the one-dimensional map to describe the equivalent form of chua's circuit, and discovered that the map's Feigenbaum constant is 4.6933[20]. Chua turned the equation which depicts the chua's circuit to three-dimensional scalar quantity differential equation, and traced the double-periodic process with the equation's result. He presented that the bifurcation series' interval rate accord with the Feigenbaum constant[21]. Wikan and his partners pointed out that Feigenbaum constant also exists in the population model[22]. Using the series arithmetic, Dooren found that there are at least six phases of double-periodic bifurcation process in the way of suppressed Duffing system to chaos, and every phase bifurcation process can be defined by the constant 4.6692[23]. Cooper researched the double-periodic bifurcation process in Carotid-Kundalini map and gravity data, and calculated the

result consistent with the Feigenbaum constant[24,25]. The above studies indicate that the general feature of double-periodic bifurcation to chaos can apply to all of nonlinear map in addition to logistic map.

(2) From Fig.3, we can see that there are δ function style sharp spikes in the fundamental frequency and its higher harmonic waves in the power spectra from Fig.3(a) to Fig.3(c). From Fig.4 we can find d=1 or 0, and λ_1 is negative in the condition mentioned above. This indicates that the movement of Eq.(2) is periodic as the fixed points and limit loop shown in from Fig.1(a) to Fig.1(c). From Fig.3(d) to Fig.3(f), the power spectra do not have sole frequency spikes only in the fundamental frequency and its higher harmonic waves but abundance frequency components and noise background for broad band. From Fig.4, we can see that the fractal dimension d of attractors of Eq.(2) shown as from Fig.1(d) to Fig.1(f) are all fractional and their maximum Lyapunov exponents λ_1 are all positive real. This indicates that Eq.(2) is chaotic, that is to say, the attractors given from Fig.1(d) to Fig.1(f) are strange attractors.

(3) The study on attraction basin of periodic orbits of the coupled logistic map indicates that the iterative result of the coupled logistic map relies on the initial value, i.e., the iteration process started from different division on (x,y) plane converges to different periodic or non-periodic orbit. In this sense, it is much different from the one-dimensional map where there is no more than one stable period and whatever the initial value is, the same result will be achieved. Moreover, the boundary between periodic and non-periodic region in attraction basin is fractal, i.e., there exists delicate structure to arbitrary minute scale.

The study on the Mandelbrot-Julia set of the coupled logistic map shows that the Mandelbrot-Julia set will be different under variable control parameters and the boundary of stable region is smooth, and it exhibits the fractal property.

References:

[1] May RM. Simple mathematical models with very complicated dynamics. Nature, 1976,261:459−467.

[2] Feigenbaum MJ. Quantitative universality for a class of nonlinear transformations. Journal of Statistical Physics, 1978,19(1):25−52.

[3] Wang XY. Chaos in the Complex Nonlinearity System. Beijing: Electronics Industry Press, 2003. 91−113 (in Chinese).

[4] Satoh K, Aihara T. Self-Similar structures in the phase diagram of a coupled-logistic map. Journal of the Physical Society of Japan, 1990,59:1123−1126.

[5] Hastings A. Complex interactions between dispersal and dynamics: Lessons from coupled logistic equations. Ecology, 1993,74(5): 1362−1372.

[6] Zengru D, Sanglier M. A two-dimensional logistic model for the interaction of demand and supply and its bifurcations. Chaos, Solitons & Fractals, 1996,7(12):2259−2266.

[7] Guckenheimer J, Holmes P. Nonlinear Oscillations, Dynamical Systems, and Bifurcations of Vector Fields. Berlin: Springer-Verlag, 1983. 156−165.

[8] Eckmann JP. Roads to turbulence in dissipative dynamics system. Reviews of Modern Physics, 1981,53:643−649.

[9] Welch PD. The use of fast Fourier transform for the estimation for the estimation of power spectra: A method based on time averaging over short, modified periodograms. IEEE Trans. on Audio and Electroacoust, 1967,15(2):70−73.

[10] Kaplan JL, Yorke JA. Chaotic behavior of multidimensional difference equations. In: Peitgen HO, Walther HO, eds. Functional Differential Equations and Approximation of Fixed Points. Lecture Notes in Mathematics 730, Berlin: Springer-Verlag, 1979. 204−227.

[11] Haken H. Advanced Synergetics. New York: Springer-Verlag, 1983. 113−176.

[12] Glass L, Mackey MC. From Clocks to Chaos. Princeton: Princeton University Press, 1988. 24−62.

[13] Wang XY. Fractal Mechanism of the Generalized M-J Set. Dalian: Press of Dalian University of Technology, 2002. 1−58 (in Chinese).

[14] Gujar UG, Bhavsar VC. Fractals from $z \leftarrow z^{\alpha}+c$ in the complex c-plane. Computers & Graphics, 1991,15(3):441−449.

[15] Gujar UG, Bhavsar VC, Vangala N. Fractals images from $z \leftarrow z^{\alpha}+c$ in the complex z-plane. Computers & Graphics, 1992,16(1): 45−49.

[16] Wang XY, Liu XD, Zhu WY, *et al*. Analysis of c-plane fractal images from $z \leftarrow z^{\alpha}+c$ for $\alpha<0$. Fractals, 2000,8(3):307−314.

[17] Rössler OE, Kahlert C, Parisi J, *et al*. Hyperchaos and Julia sets. Zeitschrift fur Naturforschung Section A-A Journal of Physical Sciences, 1986,41: 819−822.

[18] Kaneko K. Transition from torus to chaos accompanied by frequency locking with symmetry breaking. Progress of Theoretical Physics, 1983,69(5):1427−1442.

[19] Feigenbaum MJ. Universal behaviour in nonlinear system. Los Alamos Science, 1990,1:4−27.

[20] Broucke ME. One parameter bifurcation diagram for chua's circuit. IEEE Trans. on Circuits and System I-Fundamental Theory and Applications, 1987,34(2):208−209.

[21] Chua LO, Huynh LT. Bifurcation analysis of Chua's circuit. In: Proc. of the 35th Midwest Symp. on Circuits and Systems, Washington, 1992. 746−751.

[22] Wikan A, Mjølhus E. Periodicity of 4 in age-structured population models with density dependence. Journal of Theoretical Biology, 1995,173:109−119.

[23] Dooren RV, Janssen H. A continuation algorithm for discovering new chaotic motions in forced Duffing systems. Journal of Computational and Applied Mathematics, 1996,66(4):527−541.

[24] Cooper GRJ. Chaotic behaviour in the Carotid-Kundalini map function. Computers & Graphics, 2000,24(3):465−470.

[25] Cooper GRJ. Aspects of chaotic dynamics in the least-squares inversion of gravity data. Computers & Graphics, 2001,25(4):691−697.

附中文参考文献:

[3] 王兴元.复杂非线性系统中的混沌.北京:电子工业出版社,2003.91−113.

[13] 王兴元.广义 M-J 集的分形机理.大连:大连理工大学出版社,2002.1−58.

WANG Xing-Yuan was born in 1964. He is a professor and doctoral supervisor at the School of Electronic and Information Engineering, Dalian University of Technology. His current research areas are chaos-fractal theory and its application.

LUO Chao was born in 1979. He is a master candidate at the School of Electronic and Information Engineering, Dalian University of Technology. His current research areas are chaos-fractal theory and its application.